NJC

PAPER

View Article Online
View Journal | View Issue

Cite this: *New J. Chem.*, 2014, **38**, 3443

Switching off the single-molecule magnet properties of the $[Co^{II}(Me_6tren)(OH_2)]^{2+}$ module by complexation with *trans*-$[Ru^{III}(salen)(CN)_2]^-$†

Dalice M. Piñero Cruz,[ab] Daniel N. Woodruff,[ab] Ie-Rang Jeon,[ab] Indrani Bhowmick,[ab] Mihail Secu,[abc] Elizabeth A. Hillard,[ab] Pierre Dechambenoit[ab] and Rodolphe Clérac*[ab]

Received (in Montpellier, France) 25th March 2014,
Accepted 28th April 2014

DOI: 10.1039/c4nj00452c

www.rsc.org/njc

The trinuclear complex $[\{Co^{II}(Me_6tren)\}_2(\mu\text{-}NC)_2Ru^{III}(salen)](NO_3)_3\cdot 3CH_3CN\cdot H_2O$ (**2**) (salen = *N*,*N*′-ethylene-bis(salicylideneiminato); Me_6tren = tris((dimethylamino)ethyl)amine) was synthesized by the reaction of *trans*-$(PPh_4)[Ru^{III}(salen)(CN)_2]$ and two equivalents of $[Co^{II}(Me_6tren)(OH_2)](NO_3)_2$ (**1**). Magnetic susceptibility measurements of **1** reveal its single-molecule magnet behaviour whilst **2** shows no appreciable slow dynamics of the magnetization even under an applied dc field. A comparison of the electrochemical properties of complex **2** with the *trans*-$(PPh_4)[Ru^{III}(salen)(CN)_2]$ precursor reveals anodic shifts of the reduction and oxidation waves. The absorption spectrum of **2** obtained from surface optical reflectivity methods is also reported and discussed.

Introduction

With recent examples of mononuclear Co(II) and Fe(II) complexes exhibiting single molecule magnet (SMM) behaviour,[1] our group has turned its attention to complexes of the amino based chelating ligand Me_6tren.[2] This tripodal tetraamine has the advantage of restricting the coordination sites of a metal centre, acting as a capping ligand, thus allowing the formation of controlled topologies.[3–7] The Me_6tren ligand can impose a trigonal bipyramid environment around the coordinated metal centres,[7,8] which is known to be a coordination geometry that favours SMM behaviour in Co(II) complexes.[1h]

Previously, we reported a number of cyanido-based complexes linking 3d, 4d and 5d metal ions to form polynuclear complexes as well as 1- and 2-dimensional networks.[9–11] Some of these systems exhibit magnetic properties characteristic of single-chain magnets (SCMs).[10,11] In our quest for new SMM and SCM systems, we have chosen to use the *trans*-$[Ru^{III}(salen)(CN)_2]^-$ module to link mononuclear Me_6tren-based species.

trans-$[Ru^{III}(salen)X_2]^{+/0/-}$ complexes have relevance in a number of branches of coordination chemistry such as catalysis, electrochemical sensors and magnetism.[9a,12–16] Most of these complexes exhibit two reversible redox processes arising from the II–IV oxidation states in which ruthenium is stable. Over the years the effect of the axial ligands (neutral or anionic) on both the redox potentials and catalytic activity of $[Ru^{III}(salen)X_2]^{+/0/-}$ complexes has been demonstrated and studied.[15,16] Leung and Che found that the catalytic activity of *trans*-$[Ru^{III}(salen)X_2]^{+/0/-}$ complexes disappeared when X = CN^-, due to its substitutional inertness.[15] However, in the area of magnetism, having cyanido axial ligands might be beneficial as they open the possibility of coordination to other paramagnetic centres, thus providing an efficient path for magnetic coupling. Indeed, *trans*-$[Ru^{III}(salen)(CN)_2]^-$ has been used as a precursor in the synthesis of 0, 1 and 2-dimensional heteronuclear systems exhibiting interesting magnetic properties.[9a,12,13] Its use in the preparation of molecule-based magnetic materials has the advantages that it is easy to synthesize and contains a paramagnetic 4d centre that can interact with other metal centres through the cyanido groups, whose *trans*-disposition also allows extendable coordination.

Herein we present the work developed from the use of the Me_6tren capping ligand and the salt $Co^{II}(NO_3)_2\cdot 6H_2O$ to yield the $[Co^{II}(Me_6tren)(OH_2)]^{2+}$ SMM (**1**), and its coordination to the *trans*-$[Ru^{III}(salen)(CN)_2]^-$ precursor to form the trinuclear complex $[\{Co^{II}(Me_6tren)\}_2(\mu\text{-}NC)_2Ru^{III}(salen)](NO_3)_3\cdot 3CH_3CN\cdot H_2O$ (**2**) for which the SMM properties are "switched off". This new trinuclear species presents the novel structural feature of two pentacoordinate Co^{II} ions surrounding a hexacoordinated Ru^{III} ion through cyanido bridges. We here report the structural, spectroscopic, electrochemical and magnetic properties of complexes **1** and **2**.

[a] *CNRS, CRPP, UPR 8641, Laboratory for "Molecular Materials and Magnetism", F-33600 Pessac, France. E-mail: clerac@crpp-bordeaux.cnrs.fr; Fax: +33 556845600; Tel: +33 556845650*
[b] *Univ. Bordeaux, CRPP, UPR 8641, F-33600 Pessac, France*
[c] *Moldova State University, Mateevici 60, Chisinau, MD-2009, Republic of Moldova*

† Electronic supplementary information (ESI) available. CCDC 991663 and 991664. For ESI and crystallographic data in CIF or other electronic format see DOI: 10.1039/c4nj00452c

Experimental

Me_6tren and *trans*-$(PPh_4)[Ru^{III}(salen)(CN)_2]$ were synthesized according to the literature.[2,7,13,15] All the reagents used for the syntheses were purchased from commercial sources and directly handled without further purification. Complexes **1** and **2** were synthesized under argon using Schlenk techniques. Acetonitrile and diethyl ether were of reagent grade and were deoxygenated with argon before use. **Caution!** We did not encounter any problems during our studies; nevertheless, cyanido-based compounds are often toxic and should be handled with care.

Synthetic procedures

$[Co^{II}(Me_6tren)(OH_2)](NO_3)_2$ (1). 0.030 g (0.13 mmol) of Me_6tren was added to a Schlenk tube containing 0.038 g (0.13 mmol) of $Co^{II}(NO_3)_2{\cdot}6H_2O$ in 5 mL of acetonitrile. The solution was stirred for 30 min and filtered. Green single crystals suitable for X-ray diffraction were obtained after one week by Et_2O vapour diffusion. Yield: 0.046 g (80% based on Co). Anal. calcd (found) for $C_{12}H_{32}CoN_6O_7$: C: 33.41% (33.79%); H: 7.48% (7.41%); N: 19.48% (19.53%). IR/cm^{-1}: 2940 (m), 2901 (m), 1478 (m), 1467 (w), 1451 (w), 1393 (s), 1290 (s), 1249 (w), 1184 (w), 1099 (m), 1037 (m), 1016 (w), 1003 (m), 945 (m), 935 (w), 911 (w), 826 (w), 808 (w), 774 (w), 739 (w), 599 (w), 574 (w).

$[\{Co^{II}(Me_6tren)\}_2(\mu\text{-}NC)_2Ru^{III}(salen)](NO_3)_3{\cdot}3CH_3CN{\cdot}H_2O$ (2). 0.057 g (0.13 mmol) of **1** was dissolved in acetonitrile. To this solution was added 0.046 g (0.06 mmol) of *trans*-(PPh_4)-$[Ru^{III}(salen)(CN)_2]$. The reaction mixture was then stirred for 2 hours before filtration. Dark blue single crystals suitable for X-ray diffraction were obtained after two days by Et_2O vapour diffusion into the reaction mixture. Yield: 0.040 g (50% based on the Ru^{III} precursor). Anal. calcd (found) for $C_{48}H_{83}Co_2N_{18}O_{12}Ru$: C: 43.57% (43.94%); H: 6.32% (6.68%); N: 19.05% (19.49%). IR/cm^{-1}: 3424 (b), 2916 (m), 2108 (m) ($\bar{\nu}_{CN}$), 1611 (m), 1597 (w), 1530 (w), 1474 (w), 1436 (m), 1321 (s), 1286 (s), 1242 (m), 1191 (m), 1149 (m), 1130 (m), 1100 (m), 1038 (m), 1018 (m), 1003 (m), 945 (s), 935 (s), 911 (m), 899 (m), 829 (m), 805 (m), 776 (m), 756 (m), 738 (m), 720 (m), 623 (m), 600 (m), 572 (m). $\bar{\nu}_{CN}$ for the Ru^{III} precursor is at 2088 cm^{-1} (s).

Crystal structure determination

Single crystals of **1** and **2** were coated with N-paratone oil and mounted on a fibre loop. X-ray crystallographic data were collected on a Bruker APEX II Quazar diffractometer with graphite-monochromated Mo-Kα radiation (λ = 0.71073 Å) at 100(2) K. The program SAINT was used to integrate the data while the absorption correction was based on multiple and symmetry-equivalent reflections in the dataset using SADABS.[17] The structures were solved with SIR92 and refined by full-matrix least squares on F^2 using SHELXL-97.[18,19] All atoms, except hydrogen, were refined anisotropically. The H atoms were placed at calculated positions using suitable riding models except those on the coordinated water molecule, which were found directly on the difference Fourier map and refined using DFIX constraints. A summary of the crystallographic data and selected structural details (bond lengths and angles) are reported in Tables 1 and 2.

Table 1 Crystallographic data and refinement parameters for **1** and **2**

Complex	**1**	**2**
Formula	$C_{12}H_{32}CoN_6O_7$	$C_{48}H_{85}Co_2N_{18}O_{12}Ru$
FW (g mol^{-1})	431.37	1325.27
Crystal colour	Green	Dark blue
Crystal size (mm)	0.10 × 0.17 × 0.09	0.26 × 0.12 × 0.03
Crystal system	Monoclinic	Monoclinic
Space group	$P2_1$	$P2_1/c$
T (K)	100(2)	100(2)
a (Å)	9.131(3)	19.577(2)
b (Å)	12.369(4)	33.296(3)
c (Å)	9.870(4)	9.372(1)
α (°)	90	90
β (°)	117.337(13)	103.641(1)
γ (°)	90	90
V (Å^3)	990.2(6)	5937(1)
Z	2	4
Total refls	5808	10 943
Unique refls ($I > 2\sigma(I)$)	4808	8964
R_{int}	0.0615	0.0706
Refined param./restr.	247/3	745/0
$R_1(I > 2\sigma(I))$	0.0414	0.0549
wR_2 (all data)	0.1185	0.1673
Goodness-of-fit	1.099	1.133

Table 2 Selected bond lengths (Å) and angles (°) for **1** and **2**

Complex **1**		Complex **2**	
Co1–N4	2.144(12)	Ru1–N12	2.011(5)
Co1–N3	2.115(9)	Ru1–N11	2.011(4)
Co1–N2	2.136(18)	Ru1–O1	2.015(4)
Co1–N1	2.179(3)	Ru1–O2	2.017(4)
Co1–O1	2.018(3)	Ru1–C25	2.032(6)
O1–Co1–N1	177.12(10)	Ru1–C26	2.068(6)
O1–Co1–N4	99.02(11)	Co1–N9	1.997(4)
O1–Co1–N3	99.94(13)	Co1–N3	2.109(5)
O1–Co1–N2	95.17(14)	Co1–N4	2.113(4)
		Co1–N2	2.114(5)
		Co1–N1	2.194(5)
		Co2–N10	2.020(4)
		Co2–N8	2.121(5)
		Co2–N6	2.122(4)
		Co2–N7	2.126(6)
		Co2–N5	2.205(4)
		C25–Ru1–C26	178.72(24)
		N9–Co1–N1	178.28(16)
		N10–Co2–N5	177.76(17)
		N9–C25–Ru1	176.09(51)
		N10–C26–Ru1	176.14(51)
		C25–N9–Co1	171.92(44)
		C26–N10–Co2	167.64(44)

CCDC 991663 and 991664 for **1** and **2**, respectively. Fig. 1 and 2 were generated using CrystalMaker® (CrystalMaker Software Ltd, www.crystalmaker.com).

Electrochemical experiments

Cyclic voltammetry measurements were performed using a CHI 760c potentiostat, in a standard one-compartment cell under N_2, equipped with platinum wires for working/counter electrodes and a silver wire (Ag/Ag^+) for the reference electrode. Solutions were prepared from 0.1 M tetraethylammonium tetrafluoroborate ($[NEt_4^+][BF_4^-]$) in acetonitrile. Ferrocene was added at the end of each experiment and potentials are referenced to the $Cp_2Fe^{+/0}$ couple.

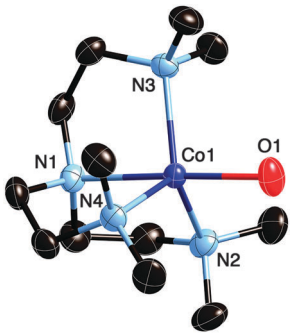

Fig. 1 ORTEP-type view of the cation as found in the crystal structure of **1** at 100 K with thermal ellipsoids at the 50% probability level. Hydrogen atoms and nitrate anions are omitted for clarity.

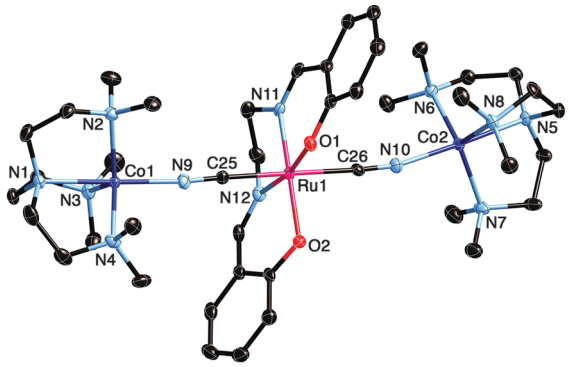

Fig. 2 ORTEP-type view of the cation as found in the crystal structure of **2** at 100 K with thermal ellipsoids at the 50% probability level. Hydrogen atoms, nitrate anions and interstitial solvent molecules are omitted for clarity.

Optical properties

Surface optical reflectivity measurements were performed on a home-built system at different temperatures ranging from 10 to 300 K. Heating and cooling rates were maintained at 4 K min^{-1} during the measurements. The setup collects the light reflected by the sample (sum of direct and diffuse reflected light), which was analysed using a high sensitivity Hamamatsu 10083CA spectrometer between 480 and 1050 nm. The spectra were compared to a white reference obtained with a NIST traceable standard for reflectance (SphereOptics, ref SG3054). The background, acquired with the light source switched off, was subtracted from all measurements. The absolute optical reflectivity can be plotted as a function of temperature, time or wavelength.

Magnetic properties

The samples were checked by X-ray diffraction prior to any magnetic measurements. Magnetic susceptibility measurements were performed using Quantum Design MPMS-XL SQUID and PPMS-9 magnetometers. The measurements were carried out on freshly filtered polycrystalline samples introduced in a polyethylene bag (3 × 0.5 × 0.02 cm). dc measurements were conducted from 300 to 1.85 K and between ±70 kOe applied dc fields. The thermal dependence of the magnetic susceptibility was measured at 1000 Oe. An *M vs. H* measurement was performed at 100 K to confirm the absence of ferromagnetic impurities. The field dependence of the magnetization was collected between 1.85 and 8 K while sweeping the magnetic field between 0 and 7 T at about 100 to 400 Oe min^{-1}. ac susceptibility experiments were realized at ac frequencies ranging from 10 to 10 000 Hz with an ac field amplitude of 1 Oe (PPMS) and from 1 to 1500 Hz with an ac field amplitude of 3 Oe (MPMS). Experimental data were corrected for the sample holder and for the diamagnetic contribution of the samples.

Results and discussion

Synthesis and structural characterization

The mononuclear complex **1** (Fig. 1) was obtained in good yield by the 1 : 1 reaction of Me_6tren with $Co^{II}(NO_3)_2{\cdot}6H_2O$ in acetonitrile. **1** crystallizes in the monoclinic space group $P2_1$ (Table 1). The Co^{II} trigonal bipyramidal coordination sites are composed of four nitrogen atoms from the Me_6tren ligand accounting for three equatorial and one of the axial positions. The three equatorial Co–N distances range from 2.115(9) to 2.144(12) Å (Table 2), while the axial Co–N distance is the longest at 2.179(3) Å. The $Co–O_{water}$ distance is 2.018(3) Å.

Complex **2** was synthesized in moderate yield by the reaction of two equivalents of **1** with one equivalent of *trans*-$[PPh_4]$-$[Ru^{III}(salen)(CN)_2]$. Dark blue crystals suitable for single crystal X-ray diffraction were obtained after one week of Et_2O vapour diffusion into the mother liquor. Complex **2** crystallizes in the monoclinic space group $P2_1/c$ (Table 1). The geometry of this trinuclear complex can be described as pseudo-linear with two $[Co^{II}Me_6tren]^{2+}$ units capping the central *trans*-$[Ru^{III}(salen)(CN)_2]^-$ building-block through Co–NC bonds (Fig. 2). Deviation from linearity is mostly found at the Co–N–C angles, with 171.9(4)° and 167.6(4)° for the Co1 and Co2 sites, respectively. Small differences in the bond distances are found between complex **2** and those of its precursors. For example, the axial $Co–N_{Me_6tren}$ distance is slightly longer than in the mononuclear complex **1** with values from Co1 and Co2 sites of 2.194(5) and 2.205(4) Å, respectively. As for the Ru^{III} site, both Ru–C distances are slightly shorter in **2** than in the precursor (2.066(3) and 2.080(3) Å),[20] with distances of 2.032(6) and 2.068(6) Å, while all equatorial positions are slightly longer (Table 2). Despite the aforementioned minor structural difference between the two Co^{II} sites in complex **2**, this dissymmetry is not distinguishable on the IR spectrum of **2**, which exhibits only one CN stretching band at 2108 cm^{-1} and no duplication of other ligand related bands.

Electrochemical properties

The redox properties of complexes **1** and **2** in acetonitrile were studied by cyclic voltammetry (Fig. S1 and S2, ESI†) and are reported *vs.* $Cp_2Fe^{+/0}$ in Table 3. The mononuclear complex **1** exhibits one irreversible oxidation wave at +0.98 V (Fig. S1, ESI†), likely corresponding to the oxidation of Co^{II} to Co^{III}. The Ru precursor, *trans*-$(PPh_4)[Ru^{III}(salen)(CN)_2]$, displays a reversible reduction at E° = −1.05 V and a reversible oxidation at E° = +0.31 V (Fig. S3, ESI†), typical of *trans*-$[Ru^{III}(salen)X_2]^-$ complexes.[15]

Table 3 Electrochemical data for **1**, **2** and *trans*-$[Ru^{III}(salen)(CN)_2]^-$ complexes

Complexes	E° (V) (*vs.* $Cp_2Fe^{+/0}$) Reduction	Oxidation	ΔE° (V)
1		*irr.*	—
2	−0.64	+0.65	1.29
trans-$(PPh_4)[Ru^{III}(salen)(CN)_2]$	−1.05	+0.31	1.36
trans-$(Bu_4N)[Ru^{III}(salen)(CN)_2]$[15]	−1.15	+0.28	1.43

Note: *irr.* stands for irreversible; Values for *trans*-$(Bu_4N)[Ru^{III}(salen)(CN)_2]$ are referenced to $Cp_2Fe^{+/0}$ according to ref. 21.

For *trans*-$(Bu_4N)[Ru^{III}(salen)(CN)_2]$, the reported potential values (E°) of $Ru^{III} \rightarrow Ru^{II}$ and $Ru^{III} \rightarrow Ru^{IV}$ are −1.15 and +0.28 V, respectively,[15] in good agreement with those (*vide supra*) obtained here from the *trans*-$[Ru^{III}(salen)(CN)_2]^-$ complex with a PPh_4^+ counter cation.

Complex **2** exhibits two redox processes, a reversible reduction at −0.64 V and a quasi-reversible oxidation at +0.65 V (Fig. S2, ESI†). The first can be assigned to the $Ru^{III} \rightarrow Ru^{II}$ reduction with a significant anodic shift in comparison with the Ru^{III} precursor, due to the presence of the electron-withdrawing Co^{II} centres. This shift, and the absence of characteristic redox waves for the Ru^{III} precursor confirms the persistence of the trinuclear complex **2** under these solution conditions. The redox feature at +0.65 V could be attributed either to the $Ru^{III} \rightarrow Ru^{IV}$ oxidation anodically shifted due to the Co^{II} centres, or to the $Co^{II/III}$ oxidation cathodically shifted due to the change in the Co coordination sphere from a neutral to an anionic axial ligand. The ΔE° calculated for the two redox processes from the Ru^{III} mononuclear complexes[15] and that of complex **2** are reported in Table 3. The similarity of these values suggests that the redox process observed at 0.63 V for **2** likely corresponds to the oxidation of the Ru^{III} centre.

Optical measurements

The spectroscopic properties of complex **2** were probed by optical reflectivity (Fig. 3) in search of a thermal or photo-induced electron transfer process from the $Co^{II} \rightarrow Ru^{III}$ centres, an inherent feature of several cyanido-bridged mixed valence heterometallic complexes.[22–24] When cooling the sample, a slight blue shift is observed from the reflectivity band at 960 nm to 890 nm; meanwhile the rest of the spectrum remains unchanged. This band shift was examined by plotting the thermal evolution of the absolute reflectivity at 920 nm (Fig. S4, ESI†) which indeed reveals a gradual increase between 300 and 10 K. This behaviour has already been reported for $(Bu_4N)[Ru^{III}(salen)(CN)_2]$.[9] Therefore, the optical modification exhibited by complex **2** can be attributed solely to the *trans*-$[Ru^{III}(salen)(CN)_2]^-$ site and not to any other electronic process occurring between the Co^{II} and the Ru^{III} centres.

Dc magnetic susceptibility measurements

The temperature dependence of the magnetic susceptibility of complexes **1** and **2** was measured under a dc field of 1000 Oe in the 1.85–300 K temperature range. The χT product plotted as a function of temperature for **1** and **2** is shown in Fig. 4. Plots of magnetisation as a function of field for **1** and **2** are shown in Fig. S5 (ESI†).

The room temperature χT product for **1** is 2.4 cm^3 K mol^{-1}, which is higher than the value of 1.875 cm^3 K mol^{-1} expected for an $S = 3/2$ spin with $g = 2$. This high value is the result of the orbital contribution typical of a high spin Co^{II} metal ion.[25] Upon decreasing temperature, the χT product remains relatively unchanged until around 15 K when a rapid decrease to a value of 1.68 cm^3 K mol^{-1} at 1.85 K is observed, as a signature of the Co^{II} spin–orbit coupling.

At room temperature, the χT value of **2** is 5.2 cm^3 K mol^{-1}, which accounts for three isolated spin centres: two high spin Co^{II} with Curie constants of about 2.4 cm^3 K mol^{-1} (on the basis of the magnetic properties of **1**, *vide supra*) and one low spin $S = 1/2$ Ru^{III} magnetic centre with a Curie constant equal to 0.4 cm^3 K mol^{-1} ($g = 2.11$).[13,20] As the temperature decreases, the χT product remains unchanged until around 60 K. Below this temperature, the χT product slightly increases to 5.3 cm^3 K mol^{-1} at 14 K before experiencing a sharp decrease to reach a value of 4.4 cm^3 K mol^{-1} at 1.85 K. The thermal behaviour of the

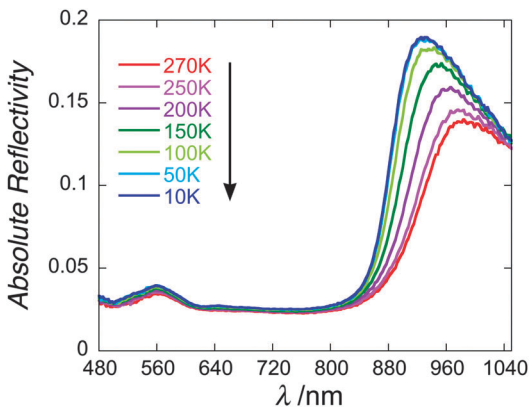

Fig. 3 Optical reflectivity spectrum of a polycrystalline sample of **2** in the 480–1050 nm spectral range at temperatures between 270 and 10 K in cooling mode (4 K min^{-1}) under spectroscopic white light (P = 0.4 mW cm^{-2}).

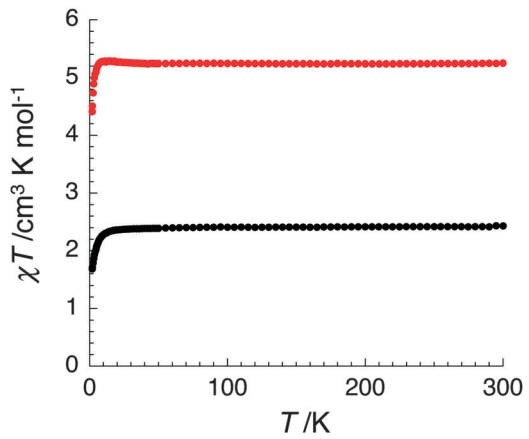

Fig. 4 Temperature dependence of the χT product (with χ defined as the molar magnetic susceptibility equal to M/H and normalized per complex) for polycrystalline samples of **1** (black) and **2** (red) at 1000 Oe.

χT product above 14 K suggests the presence of weak ferromagnetic interactions between Ru^{III} and Co^{II} magnetic sites mediated by the cyanido bridges. On the other hand below 14 K, weak intermolecular antiferromagnetic interactions and/or Co^{II} spin–orbit coupling effects are likely responsible for the decrease of the χT product.

Ac magnetic susceptibility measurements

Alternating current (ac) magnetic susceptibility measurements were performed on samples of both **1** and **2** at temperatures below 10 K. Neither complex showed an out-of-phase ac response in the zero applied field. However upon application of an external field above 200 Oe, complex **1** showed a high frequency relaxation mode at temperatures below 4 K.

The optimum field for **1** was determined by plotting curves of χ'' against frequency at 1.9 K with the application of different magnetic fields up to 7000 Oe (Fig. S6, ESI†). In the absence of a relaxation mode maximum, the optimum field was estimated at 1400 Oe, where the relaxation mode is the most intense. The temperature and frequency dependence of the ac susceptibility were thus measured at 1400 Oe (Fig. 5). Due to the absence of any maxima in the isothermal χ'' *vs.* ν plots, a standard scaling method (inset Fig. 5)[26] was used to estimate the temperature dependence of the magnetization relaxation time. Above 2.8 K, the relaxation time follows an Arrhenius law (Fig. 6) with $\Delta_{eff}/k_B = 18$ K and $\tau_0 = 9.6 \times 10^{-9}$ s. The values of Δ_{eff}/k_B and τ_0 obtained for **1** are comparable to those reported in the literature for other mononuclear Co^{II} SMMs.[1b,e–l] As expected for SMMs, τ deviates below 2.8 K from the thermally activated regime and experiences the crossover toward a relaxation regime controlled by the quantum tunnelling of the magnetization.

In contrast, for the trinuclear $[Co^{II}_2Ru^{III}]^{3+}$ complex **2**, no appreciable ac signal could be detected even in the presence of a large magnetic field (Fig. S7, ESI†). Unfortunately, this result shows that the SMM properties of **1** are lost when the $[Co^{II}Me_6tren]^{2+}$ units assemble around the *trans*-$[Ru^{III}(salen)(CN)_2]^-$ moiety.

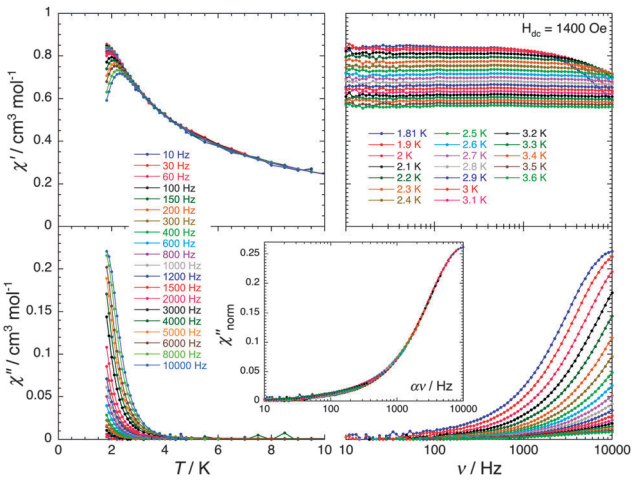

Fig. 5 Temperature (left) and frequency (right) dependence of the real (χ', top) and imaginary (χ'', bottom) parts of the ac susceptibility, between 10 and 10 000 Hz and between 1.81 and 10 K, respectively, for **1** in the 1400 Oe dc-field (with H_{ac} = 1 Oe). Solid lines are visual guides. Inset: scaled frequency dependence of χ'' (shown in the bottom left part of the main figure) normalized by the zero-frequency χ' (taken experimentally at 10 Hz) at different temperatures between 1.81 and 3.3 K (with H_{ac} = 1 Oe and H = 1400 Oe) for **1**. The scaling parameter, α, is equal to 1 for the data at 1.81 K.

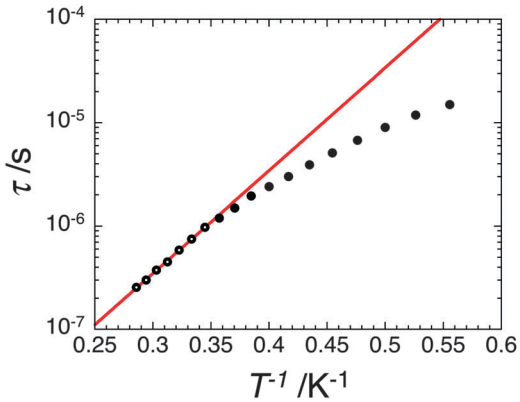

Fig. 6 τ *vs.* T^{-1} plot for **1** in 1400 Oe. Solid line is the best fit to the Arrhenius law above 2.8 K as discussed in the text.

Conclusions

We have shown that a mononuclear Co^{II} complex of Me_6tren exhibits SMM properties with an energy barrier of about 18 K. Complex **1** is another example of the ever-expanding library of mononuclear pentacoordinate Co^{II} complexes that show SMM behaviour. Two units of **1** can be linked through a *trans*-$[Ru^{III}(salen)(CN)_2]^-$ anion to form the trinuclear complex **2**, which does not exhibit SMM properties even under dc field. Complex **2** presents structural and optical properties similar to those of its precursors. However, the electrochemical properties of complex **2** are distinguishably different from those of the Co^{II} and Ru^{III} precursors at both reduction and oxidation processes. These results echo what has been reported for cyanido-bridged complexes containing Co^{II} and Ru^{III} centres bearing weak ferro- or antiferromagnetic coupling.[27–29] Work is currently underway to expand this area of research into other transition metals such as Fe(II).

Acknowledgements

We thank the Centre National de la Recherche Scientifique (CNRS), the Conseil Regional d'Aquitaine, the University of Bordeaux and the ANR for financial support. We are also grateful to Prof. Talal Mallah and Dr. Luke Batchelor for fruitful discussions about the synthesis of Me_6tren complexes. We would also like to thank Dr. Céline Pichon who initiated the synthesis of the Ru^{III} complexes.

References

1 (*a*) D. Weismann, Y. Sun, Y. Lan, G. Wolmershauser, A. K. Powell and H. Sitzmann, *Chem. – Eur. J.*, 2011, **17**, 4700–4704; (*b*) J. M. Zadrozny, J. Liu, N. A. Piro, C. J. Chang, S. Hill and J. R. Long, *Chem. Commun.*, 2012, **48**, 3927–3929; (*c*) J. M. Zadrozny, M. Atanasov, A. M. Bryan, C.-Y. Lin,

B. D. Rekken, P. P. Power, F. Neese and J. R. Long, *Chem. Sci.*, 2013, **4**, 125–138; (*d*) P.-H. Lin, N. C. Smythe, S. I. Gorelsky, S. Maguire, N. J. Henson, I. Korobkov, B. L. Scott, J. C. Gordon, R. T. Baker and M. Murugesu, *J. Am. Chem. Soc.*, 2011, **133**, 15806–15809; (*e*) T. Jurca, A. Farghal, P.-H. Lin, I. Korobkov, M. Murugesu and D. S. Richeson, *J. Am. Chem. Soc.*, 2011, **133**, 15814–15817; (*f*) J. M. Zadrozny and J. R. Long, *J. Am. Chem. Soc.*, 2011, **133**, 20732–20734; (*g*) J. Vallejo, I. Castro, R. Ruiz-García, J. Cano, M. Julve, F. Lloret, G. De Munno, W. Wernsdorfer and E. Pardo, *J. Am. Chem. Soc.*, 2012, **134**, 15704–15707; (*h*) S. Gomez-Coca, E. Cremades, N. Aliaga-Alcalde and E. Ruiz, *J. Am. Chem. Soc.*, 2013, **135**, 7010–7018; (*i*) J. M. Zadrozny, J. Telser and J. R. Long, *Polyhedron*, 2013, **64**, 209–217; (*j*) W. Huang, T. Liu, D. Wu, J. Cheng, Z. W. Ouyang and C. Duan, *Dalton Trans.*, 2013, **42**, 15326–15331; (*k*) F. Habib, O. R. Luca, V. Vieru, M. Shiddiq, I. Korobkov, S. I. Gorelsky, M. K. Takase, L. F. Chibotaru, S. Hill, R. H. Crabtree and M. Murugesu, *Angew. Chem., Int. Ed.*, 2013, **52**, 11290–11293; (*l*) E. Colacio, J. Ruiz, E. Ruiz, E. Cremades, J. Krzystek, S. Carretta, J. Cano, T. Guidi, W. Wernsdorfer and E. K. Brechin, *Angew. Chem., Int. Ed.*, 2013, **52**, 9130–9134; (*m*) J. M. Zadrozny, D. J. Xiao, J. R. Long, M. Atanasov, F. Neese, F. Grandjean and G. J. Long, *Inorg. Chem.*, 2013, **52**, 13123–13131; (*n*) A. Eichhöfer, Y. Lan, V. Mereacre, T. Bodenstein and F. Weigend, *Inorg. Chem.*, 2014, **53**, 1962–1974; (*o*) Y.-Y. Zhu, C. Cui, Y.-Q. Zhang, J.-H. Jia, X. Guo, C. Gao, K. Qian, S.-D. Jiang, B.-W. Wang, Z.-M. Wang and S. Gao, *Chem. Sci.*, 2013, **4**, 1802–1806.

2 M. Ciampolini and N. Nardi, *Inorg. Chem.*, 1966, **4**, 41–44.

3 E. G. Tulsky, N. R. Crawford, S. A. Baudron, P. Batail and J. R. Long, *J. Am. Chem. Soc.*, 2003, **125**, 15543–15553.

4 W. G. Jackson, A. M. Sargeson, P. A. Tucker and A. D. Watson, *J. Am. Chem. Soc.*, 1981, **103**, 533–540.

5 J.-Z. Gu, H.-Z. Kou, L. Jiang, T.-B. Lu and M.-Y. Tan, *Inorg. Chim. Acta*, 2006, **359**, 2015–2022.

6 S. Utsuno, H. Miyamae, S. Horikoshi and I. Endo, *Inorg. Chem.*, 1985, **24**, 1348–1354.

7 (*a*) G. J. Britovsek, J. England and A. J. White, *Inorg. Chem.*, 2005, **44**, 8125–8134; (*b*) R. Ruamps, R. Maurice, L. Batchelor, M. Boggio-Pasqua, R. Guillot, A. L. Barra, J. Liu, E.-E. Bendeif, S. Pillet, S. Hill, T. Mallah and N. Guihéry, *J. Am. Chem. Soc.*, 2013, **135**, 3017–3026.

8 U. Baisch and R. Poli, *Polyhedron*, 2008, **27**, 2175–2185.

9 (*a*) C. Pichon, P. Dechambenoit and R. Clérac, *Polyhedron*, 2013, **52**, 476–481; (*b*) A. Panja, P. Guionneau, I.-R. Jeon, S. M. Holmes, R. Clérac and C. Mathonière, *Inorg. Chem.*, 2012, **51**, 12350–12359; (*c*) T. Senapati, C. Pichon, R. Ababei, C. Mathonière and R. Clérac, *Inorg. Chem.*, 2012, **51**, 3796–3812; (*d*) R. Ababei, C. Pichon, O. Roubeau, Y.-G. Li, N. Bréfuel, L. Buisson, P. Guionneau, C. Mathonière and R. Clérac, *J. Am. Chem. Soc.*, 2013, **135**, 14840–14853; (*e*) I.-R. Jeon, S. Calancea, A. Panja, D. M. Pinero Cruz, E. S. Koumousi, P. Dechambenoit, C. Coulon, A. Wattiaux, P. Rosa, C. Mathonière and R. Clérac, *Chem. Sci.*, 2013, **4**, 2463–2470; (*f*) I. Bhowmick, T. D. Harris, P. Dechambenoit, E. A. Hillard, C. Pichon, I.-R. Jeon and R. Clérac, *Sci. China: Chem.*, 2012, **55**, 1004–1011.

10 I. Bhowmick, E. A. Hillard, P. Dechambenoit, C. Coulon, T. D. Harris and R. Clérac, *Chem. Commun.*, 2012, **48**, 9717–9719.

11 (*a*) T. D. Harris, M. V. Bennett, R. Clérac and J. R. Long, *J. Am. Chem. Soc.*, 2010, **132**, 3980–3988; (*b*) H. Miyasaka, T. Madanbashi, A. Saitoh, N. Motokawa, R. Ishikawa, M. Yamashita, S. Bahr, W. Wernsdorfer and R. Clérac, *Chem. – Eur. J.*, 2012, **18**, 3942–3954.

12 J. A. Duimstra, C. L. Stern and T. J. Meade, *Polyhedron*, 2006, **25**, 2705–2709.

13 W.-F. Yeung, P.-H. Lau, T.-C. Lau, H.-Y. Wei, H.-L. Sun, S. Gao, Z.-D. Chen and W.-T. Wong, *Inorg. Chem.*, 2005, **44**, 6579–6590.

14 W.-L. Man, H.-K. Kwong, W. W. Y. Lam, J. Xiang, T.-W. Wong, W.-H. Lam, W.-T. Wong, S.-M. Peng and T.-C. Lau, *Inorg. Chem.*, 2008, **47**, 5936–5944.

15 W. H. Leung and C. M. Che, *Inorg. Chem.*, 1989, **28**, 4619–4622.

16 M. Reza-Ganjali, M. Reza-Pourjavid, M. Rezapour, T. Poursaberi, A. Daftari and M. Salavati-Niasari, *Electroanalysis*, 2004, **16**, 922–927.

17 G. M. Sheldrick, *SADABS Version 2.03*, Bruker Analytical X-Ray Systems, Madison, WI, 2000.

18 G. M. Sheldrick, *SHELXL-97 Program for Crystal Structure Refinement*, University of Göttingen, Göttingen, Germany, 1997.

19 A. Altomare, G. Cascarano, C. Giacovazzo, A. Guagliardi, M. C. Burla, G. Polidori and M. Camalli, *J. Appl. Crystallogr.*, 1994, **27**, 435–436.

20 I. Bhowmick, PhD thesis, University of Bordeaux, 2011.

21 *Handbook of Electrochemistry*, ed. C. G. Zoski, Elsevier BV, Amsterdam, 2007, ch. 4, p. 102.

22 P. V. Bernhardt, F. Bozoglian, B. P. Macpherson and M. Martinez, *Coord. Chem. Rev.*, 2005, **249**, 1902–1916.

23 A. Bleuzen, V. Marvaud, C. Mathonière, B. Sieklucka and M. Verdaguer, *Inorg. Chem.*, 2009, **48**, 3453–3466.

24 D. Li, R. Clérac, O. Roubeau, E. Harté, C. Mathonière, R. Le Bris and S. M. Holmes, *J. Am. Chem. Soc.*, 2008, **130**, 252–258.

25 (*a*) F. E. Mabbs and D. J. Machin, *Magnetism and Transition Metals Complexes*, Chapman and Hall Ltd, London, 1973; (*b*) R. L. Carlin, *Magnetochemistry*, Springer-Verlag, Berlin, Heidelberg, 1986.

26 A. Labarta, O. Iglesias, L. Balcells and F. Badia, *Phys. Rev. B: Condens. Matter Mater. Phys.*, 1993, **48**, 10240–10246.

27 J. Xiang, W.-L. Man, J. Guo, S.-M. Yiu, G.-H. Lee, S.-M. Peng, G. Xu, S. Gao and T.-C. Lau, *Chem. Commun.*, 2010, **46**, 6102–6104.

28 J. Xiang, L.-H. Jia, W.-L. Man, K. Qian, S.-M. Yiu, G.-H. Lee, S.-M. Peng, S. Gao and T.-C. Lau, *Chem. Commun.*, 2011, **47**, 8694–8696.

29 L. M. Toma, L. D. Toma, F. S. Delgado, C. Ruiz-Pérez, J. Sletten, J. Cano, J. M. Clemente-Juan, F. Lloret and M. Julve, *Coord. Chem. Rev.*, 2006, **250**, 2176–2193.